

## Chapter 2

# Organic Nanomaterials with Two-Photon Absorption Properties for Biomedical Applications

Laura Aparicio-Ixta, Mario Rodriguez and Gabriel Ramos-Ortiz

**Abstract** During recent years there have been notorious advances in the development of organic molecules and  $\pi$ -conjugated polymers with two-photon activity, i.e., emission of fluorescence promoted by the molecular absorption of two photons. Novel organic materials have reached very large two-photon activity, and many of them have been processed successfully into nanostructured platforms. In contrast to their inorganic counterpart, organic nanoparticles with photonic properties is a topic that so far has not been well explored, although deserves big potential in biomedical applications. This chapter presents recent advances in this field, particularly, in the use of organic nanoparticles as contrast agents to obtain bioimages.

## 2.1 Introduction

In the last two decades organic molecules have emerged as interesting active materials for diverse applications. When these molecules comprise  $\pi$ -conjugated systems their optical and electric properties can be enhanced. One of the most useful optical properties exhibited by these molecules is the two-photon absorption (TPA) process.

The number of organic compounds that exhibit TPA have increased rapidly in recent years, with a variety of photonic and biological applications such as two-photon laser scanning microscopy [1], frequency upconversion lasing [2, 3], optical power limiting [4], 3-D microfabrication [5], high density optical storage [6], sensors [7] and photodynamic therapy [8, 9]. Among these applications, two-photon laser scanning microscopy, or simply two-photon microscopy (TPM) has gained great acceptance in biomedical community as a tool able to provide direct observation of cells or subcellular structures, tissue and biological processes. This technique is based in the use of molecules that exhibit strong luminescence induced by

---

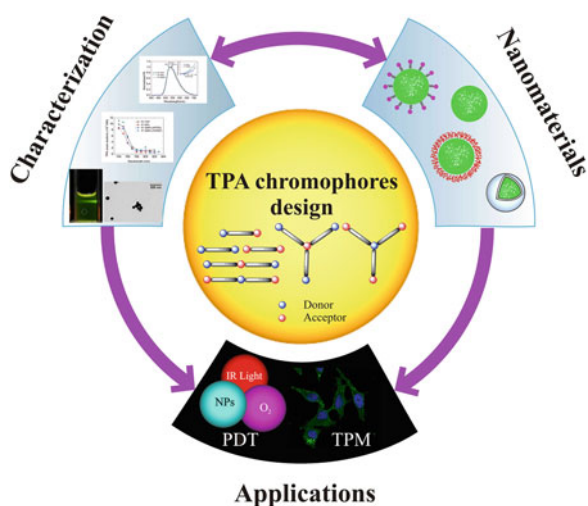
L. Aparicio-Ixta · M. Rodriguez · G. Ramos-Ortiz (✉)  
Centro de Investigaciones en Óptica A.C., A.P. 1-948, 37000 León, Guanajuato, Mexico  
e-mail: garamoso@cio.mx

TPA and offers several advantages such as high resolution, high penetration depth in tissue, weak photobleaching and weak autofluorescence, minimal phototoxicity and excitation confinement exclusively to the focal plane.

This chapter will cover recent advances in organic materials with TPA and fluorescent properties and how they can be processed into different platforms, i.e., nanostructures, in order to confer them utility in biomedical applications. Figure 2.1 presents schematically the approach followed in this field, which consists in the development of novel organic molecular systems, the subsequent characterization of their nonlinear optical properties, and the methodologies to process them and confer them enough biocompatibility to be inserted on biological media. This chapter presents information on organic nanoparticles with luminescent and nonlinear absorption properties intended to obtain bio-images by using TPM. This type of microscopy technique was reported nearly twenty five year ago and it utilizes the localized luminescence induced by nonlinear absorption [1]. So far, TPM utilizes commercially available contrast agents or markers, but these are dyes with rather weak TPA activity. This opens the opportunity to develop novel contrast agents or markers based nanostructured organic materials, with enhanced optical characteristics and multifunctionality.

It should be noted that organic nanoparticles is a topic which has not been explored so extensively as their inorganic counterpart (metallic, semiconductor and metallic oxide nanoparticles). The good luminescent and nonlinear properties, combined with low cost, less toxicity than inorganics and relatively easy synthesis, makes that of organic nanoparticles deserve enormous potential in biomedical applications such as TPM. To further exemplify the use of TPA activity in organics, this chapter will also cover partially photodynamic therapy (PDT) which is utilized for the treatment of cancer.

**Fig. 2.1** Scheme followed in the development of organic nanomaterial with TPA properties and their application in two-photon microscopy (TPM) and two-photon photodynamic therapy (PDT)



## 2.2 Two-Photon Absorption Process

The molecular TPA property is defined as the electronic excitation that is induced by a simultaneous absorption of a pair of photons with the same or different energy (Fig. 2.2). This phenomenon was first predicted in 1931 by Göppert-Mayer [10] who calculated the transition probability for the absorption of two quanta of energy. In this process a photon first interacts with the molecule and promotes a transition from ground state to a temporary virtual state of higher energy. This is not a real state of the molecule and it exists only for a short time interval ( $\sim 10^{-15}$ – $10^{-16}$  s for photon energies in the visible and near-IR ranges) [11]. If during this interval of time other photon interacts with the molecule, the excited state can be achieved. The adjective “simultaneous” for TPA is used to indicate that the two photons interact with the molecule within the interval of time above mentioned and that no real states act as intermediate states in this process.

The TPA is a third-order non-linear optical process whose magnitude is proportional to the square of the light intensity. The magnitude of TPA can be quantified by introducing the parameter called TPA *cross section* ( $\sigma_{TPA}$ ). This parameter is usually expressed in Goppert-Mayer units:  $1 \text{ GM} = 10^{-50} \text{ cm}^4 \text{ s/photon}$ . Several techniques have been used to measure the two-photon excitation cross sections of various materials for more than two decades. The two main techniques for measuring  $\sigma_{TPA}$  are Z-scan [12–14] and two-photon excited fluorescence (TPEF) [15], although exist others methods as thermal lensing [16, 17] and photoacoustic measurements [18].

Z-scan is a direct method to determine the non-linear absorption in bulk materials [12–14]; this technique consists in monitoring the transmittance of the sample under test as a function of the incident intensity of a laser beam. In the practice this can be achieved by varying the position Z of the sample in the vicinity of a focused Gaussian beam, hence the term “Z-scan”. See Fig. 2.3. The Z-scan curve obtained is

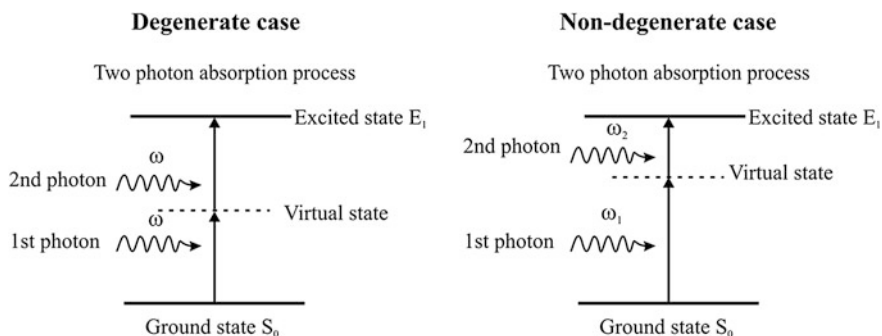


**Fig. 2.2** Schematic energy level diagram showing the excitation process of a molecule from the ground state,  $S_0$ , to an excited state,  $E_1$ . The photons can have the same energy (*degenerate case*), or different energies (*non-degenerate case*)

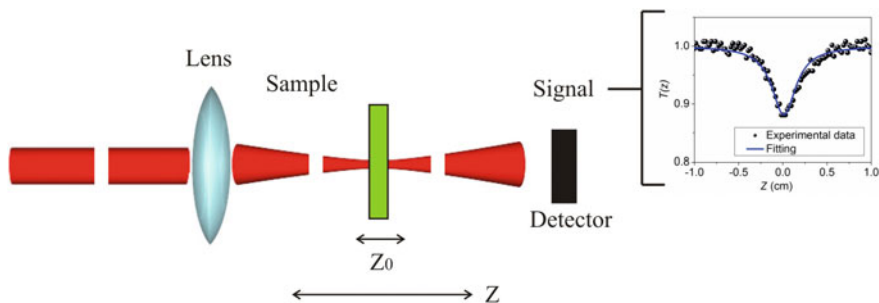


**Fig. 2.3** Z-scan technique. The energy of a train of pulses is kept constant, but changes in intensity are achieved by moving the sample along the direction  $Z$ . The transmittance is measured at each  $z$  position of the sample

symmetrical with respect to the focus ( $z = 0$ ), with a minimum in the transmittance (multiphoton absorption). The normalized transmittance is given by:

$$T(z) = 1 - \frac{1}{2^{3/2}} \sigma_{TPA} \frac{CN_A}{\hbar\omega} \frac{I_0 L_{eff}}{1 + \left(\frac{z}{z_0}\right)^2},$$

where  $C$  is the concentration of the material (usually organic materials are characterized in solution),  $N_A$  is Avogadro's number,  $\omega$  is the optical frequency of the laser,  $z_0$  the Rayleigh range of the beam,  $I_0$  the peak intensity at  $z = 0$  and  $L_{eff}$  the effective thickness of sample. With this technique  $\sigma_{TPA}$  is determined straightforwardly when short laser pulses (femtosecond or picosecond) are employed by just fitting experimental data to the expression given above. The use of nanosecond pulses can lead to an overestimation for the  $\sigma_{TPA}$  since other effect different than simultaneous TPA can also be present.

The TPEF technique is another procedure for determining  $\sigma_{TPA}$  and consists in measuring the fluorescence signal generated from a solution of the material under tests after it is excited by TPA. From the two-photon fluorescence signal a TPE (two-photon fluorescence excitation) cross section  $\sigma_{TPE}$  can be determined. A representative experimental setup is showed in Fig. 2.4. The  $\sigma_{TPE}$  is linearly proportional to  $\sigma_{TPA}$  with the constant of proportionality being the fluorescence quantum yield ( $\eta$ ) of the sample  $\sigma_{TPE} = \eta \sigma_{TPA}$ .

Some variants of this experiment have been developed since it was first reported by the Group of Webb [15, 19]. However, if a standard calibration sample of known  $\sigma_{TPE}$  and spectra is available, then the simplest approach is to compare the two-photon excited fluorescence spectra of the sample with the reference sample tested under identical conditions. With this method is possible to cancel automatically a large number of variables. For instance, it is not necessary to know parameters related to the excitation (pulse energy, pulse duration, and temporal intensity distribution) [20]. The equation to calculate the TPA cross section is given by:

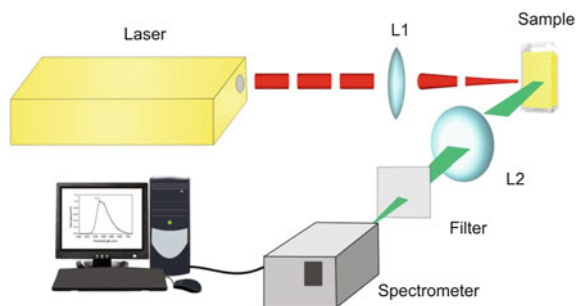


**Fig. 2.4** Typical TPEF experimental setup to measure the  $\sigma_{TPA}$  in organic materials. The photoluminescence promoted by the absorption of two photons in a solution of the material under test is detected and compared with that from a standard tested under the same experimental conditions

$$\sigma_{TPA}(\lambda) = \sigma_{TPA(ref)}(\lambda) \frac{\eta_{ref}(\lambda) C_{ref}}{\eta(\lambda) C} \frac{\langle F(t) \rangle}{\langle F(t) \rangle_{ref}} \frac{n_{ref}}{n},$$

where  $C$  denotes the concentration of solution,  $\langle F(t) \rangle$  is the time averaged fluorescence emission,  $n$  is the refractive index of the sample, and  $\lambda$  is the excitation wavelength. The subindex *ref* denotes the parameters for the dye used as reference or standard.

The principal drawback of the TPEF method is that it cannot be used for non-fluorescing or weakly fluorescing materials. TPEF is also difficult to implement in compounds that exhibit wavelength-dependent emission (in either band shape or efficiency) or dual emission, as well as in solid-state samples. In those cases the use of Z-scan is more convenient.

A wide range of organic molecules with large TPA activity have been studied experimentally employing Z-scan and TPEF techniques. In the following section we present some representative samples.

### 2.3 Design Strategies and Structure–Property Relationships for Organic Molecules

Many organic molecules and polymers having electronic  $\pi$ -conjugated systems in their structure have showed large nonlinear optical properties. So far, the largest values of  $\sigma_{TPA}$  reported in the literature are in the range of  $10^2$ – $10^4$  GM. The number of examples within this range of nonlinearities has increased notably during the last three lustrums, and scientists have designed different family of molecules to achieve these values. A large number of scientific articles that report new TPA organic fluorescent materials are oriented toward the *in vivo* or *in vitro* imaging of bio specimens, as well as the diagnosis of diseases. For these applications it is

necessary to have organic molecules with high quantum yield and large TPA cross section values, in addition to low cell-toxicity and compatibility with aqueous media. In particular, the architecture of organic molecules that have been investigated for their two-photon absorption and fluorescent properties could be classified in two principal groups: (a) linear and (b) two-dimensional architectures. For both structures there are some requirements for maximizing the TPA cross-section response: a long conjugated  $\pi$ -backbone system with a planar conformation; the presence of electron-donor (D) and electron-acceptor (A) groups able to promote an intense displacement of charge during the transition from the donor-centered HOMO (highest occupied molecular orbital) to the acceptor-centered LUMO (lowest unoccupied molecular orbital) [20]. The energy difference between the HOMO and LUMO is the optical gap corresponding to the excitation transition promoted by TPA. Depending on symmetry of the organic molecule, this gap can be the same or different than that promoted by one photon transition (linear absorption). For instance, in centrosymmetric molecules the maximum TPA usually appears at higher energies than the peak corresponding to the one-photon absorption transition. This is because one-photon and two-photon transitions are regulated by different dipole selection rules.

In the case of organic chromophores with linear architecture, including polymers and small molecules, effective molecular architectures have been used to enhance the two-photon absorption. Arrangement such as donor-bridge-acceptor ( $D-\pi-A$ ) dipolar structures (Fig. 2.5a), donor-bridge-donor ( $D-\pi-D$ ), acceptor-bridge-acceptor ( $A-\pi-A$ ), donor-acceptor-donor ( $D-\pi-A-\pi-D$ ) and acceptor-donor-acceptor ( $A-\pi-D-\pi-A$ ), the latter four corresponding to quadrupolar structures (Fig. 2.5b, c), have been designed and synthesized [21–23]. In this context the term bridge refers to a  $\pi$ -backbone system. The appropriate donor-acceptor architecture in organic  $\pi$ -systems can enhance the TPA activity through an increase in the transition dipole moment or the dipole moment difference between the ground state and excited state. Experiments indicate that quadrupolar architectures in some cases are more efficient than dipolar ones. For quadrupolar systems the best results have been obtained for architectures containing D groups in the periphery and A in the core. For molecules that possess two dimensional structures the best results correspond to architectures containing an A group in the core and D groups in a multi-branched configuration (Fig. 2.5d). These type of structures have octupolar response  $A-(\pi-D)_3$ . Typical D groups are amino moieties as diphenylamino

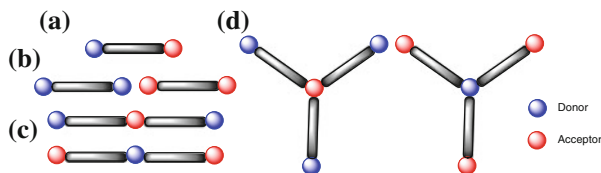


**Fig. 2.5** Molecular architectures for the optimization of TPA responses in organic compounds: **a** dipolar, **b, c** quadrupolar, **d** octupolar

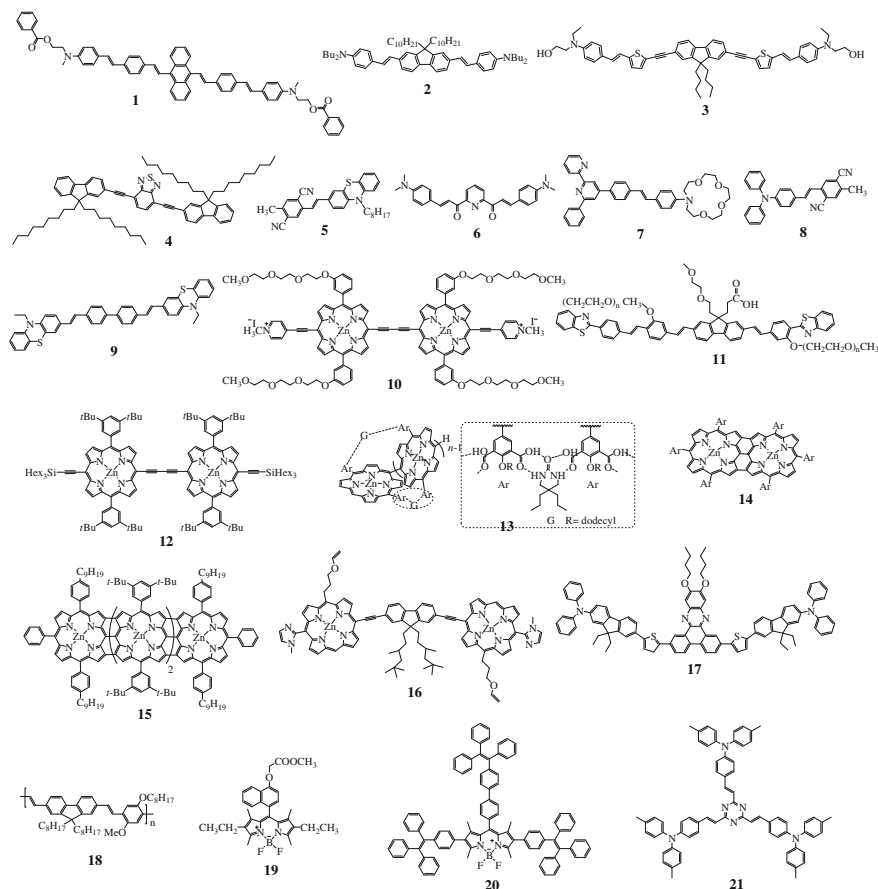


**Fig. 2.6** Linear structures of organic molecules with high TPA properties

(NPh<sub>2</sub>), dimethylamino (NMe<sub>2</sub>) or diethylamino (NEt<sub>2</sub>) which are the most employed, while some of the fragments used as A are anthracene, fluorine, benzo-thiadiazole, triazine, porphyrine or bodipys derivatives. For the  $\pi$ -bridge between D and A is common to utilize aromatic (phenyl or fluorene) or heteroaromatic rings (thiophene) to favor the planar structure. However, some reports indicate that carbon triple bond is also an excellent  $\pi$ -bridge. Figures 2.6 and 2.7 presents examples of organic molecular systems with dipolar, quadrupolar and octupolar character. These organic systems include fluorene based molecules and polymers, porphyrines, bodipy's, dendrimers, etc. and have large TPA activity with linear (Fig. 2.6) and two-dimensional (Fig. 2.7) designs.

Upon excitation, molecules with TPA properties undergo substantial intramolecular charge transfer (ICT) over the  $\pi$ -backbone. Enhancement of the  $\sigma_{TPA}$  is achieved with a correct design of the molecular structure able to modify properly the ICT. The environment is a factor that can affect the ICT process and in turn the

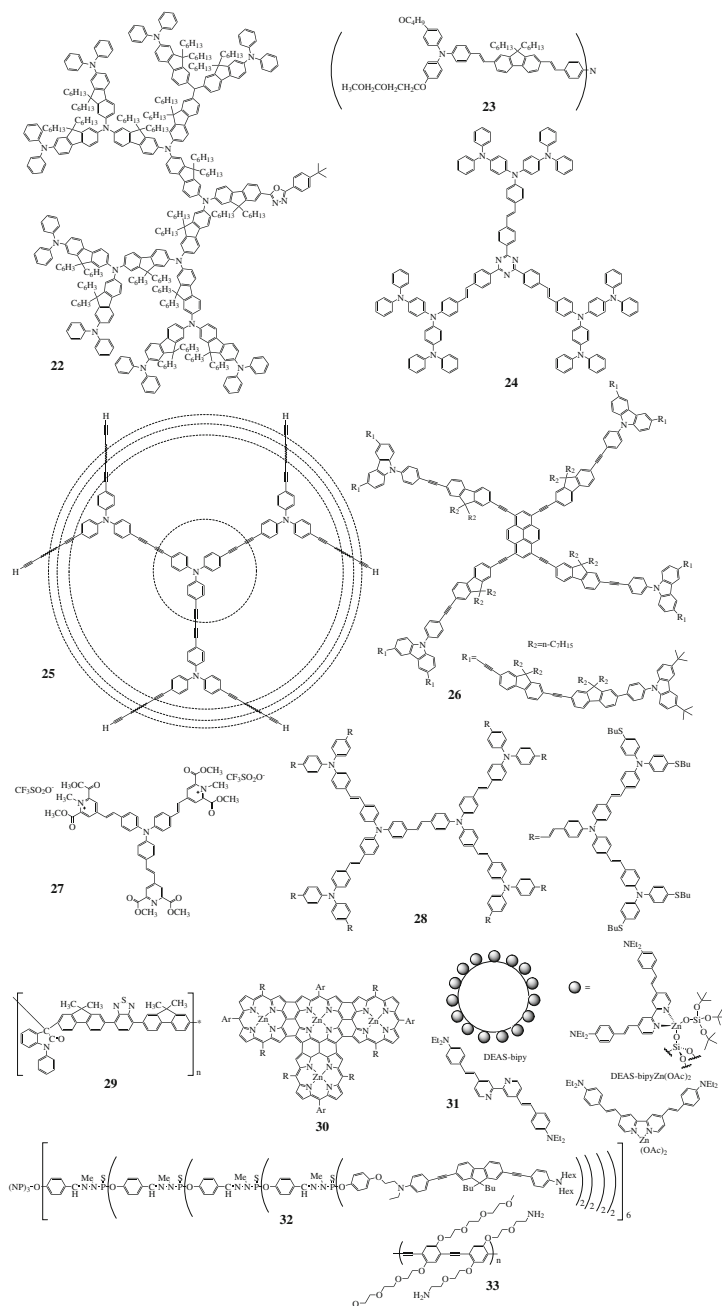


**Fig. 2.7** Two-dimensional structures of organic molecules with TPA properties



nonlinear optical response. For instance, the linear TPA dye **8** having dipolar architecture showed intense solvatochromic effect such that in cyclohexane (non-polar solvent) solution exhibits a large  $\sigma_{TPA}$  value of 6670 GM which is reduced in DMF (high polar solvent) to 1450 GM. In low polar solvents, such as toluene, the linear quadrupolar structure **17** showed  $\sigma_{TPA}$  of 7080 GM while the two-dimensional molecule **23** has an acceptable  $\sigma_{TPA}$  of 5300 GM. Other two-dimensional structures show much higher optical nonlinearities than linear structures. Examples of the latter are polymers with quadrupolar architectures (**29**) and dendrimers (**32**) which in different solvents exhibit interesting values of 9860 and 56,000 GM, respectively.

It must be observed that in general the organic molecules are hydrophobic and soluble only in highly toxic solvents. To emphasize this fact, Table 2.1 summarizes the main optical properties of the molecules shown in Figs. 2.6 and 2.7 and the cases in which the molecules can be processed into nanoparticles (NPs) susceptible to be suspended in biocompatible media, i.e., aqueous solutions. Also, as a reference, the Table 2.1 includes the nonlinear optical properties of representative inorganic nanomaterials, i.e., quantum dots (QD) and gold nanorods which are also being studied extensively in the literature for biomedical applications.

Usually organic molecules and polymers, as those shown in Figs. 2.6 and 2.7, exhibit one-photon excitation (linear absorption) in the UV-Vis of the spectrum. Accordingly, their maximum two-photon excitation (assuming that the peak of the two-photon absorption spectrum is located at twice the wavelength of the one-photon absorption) occurs in the Vis-IR range. For biomedical applications, the interest is focused in molecules with TPA in the red and near-infrared region (650–1000 nm). Effective two-photon excitation at this range of wavelengths is observed with organics with relative small optical band gap. Further, the effectiveness in nonlinear absorption must be accompanied by a second molecular functionality. For instance, when a molecule or polymer is intended as a fluorescent label or contrast agent in multiphoton microscopy, it needs to exhibit a large value of quantum yield,  $\eta$ . This is not always achieved, as it can be observed in Table 2.1. Sometimes, large  $\sigma_{TPA}$  values are obtained in detriment of  $\eta$ . In these cases, or in other cases where the needed functionality is other than fluorescence, the energy transfer concept can work satisfactorily. For instance, an effective fluorescent dye (energy acceptor) with poor two-photon activity is indirectly excited through resonant energy transfer from an effective TPA dye unit (energy donor). This concept will be further exemplified in the last section of this chapter for the application of photodynamic therapy.

## 2.4 Methods Used to Incorporate TPA Materials in Aqueous Suspensions

As mentioned in the previous section, intense studies have been focused on developing efficient TPA organic molecules that can be excited in the 650–1000 nm region, since they deserve potential application in two-photon microscopy

**Table 2.1** TPA properties of organic materials shown in Figs. 2.6 and 2.7

Organic Material	Quantum yield ( $\eta$ )	$\sigma_{\text{TPA}}$ (solution) GM/technique	$\sigma_{\text{TPA}}$ (NPs) GM	Reference
<i>Linear structures</i>				
1	0.025 (in solution) 0.13 (NPs)	172/Nonlinear transmission	217	[39]
2	1 (solution) 0.49 (SNPs)	$\sim 400$ /TPEF	–	[59]
3	0.65 (solution) 0.28 (SNPs)	1200/TPEF	1000	[37]
4	0.87 (solution) 0.83 (NPs)	1000/TPEF	514	[30]
5	0.03 (solution)	2800/TPEF	–	[76]
6	0.082 (solution)	5250/TPEF	–	[77]
7	0.027 (solution)	5956/TPEF	–	[78]
8	0.805 (solution)	6670/TPEF	–	[79]
9	0.61 (solution)	10,870/Z-scan	–	[80]
10	–	17,000/TPEF	–	[81]
11	$\sim 0.5$ (aqueous solution) 1.0 (ACN solution)	3000 ACN/TPEF $\sim 6000$ Water/TPEF		[82]
12	–	9100/Z-scan	–	[83]
13	–	13,200/Z-scan	–	[83]
14	–	41,200/Z-scan	–	[83]
15	–	93,600/Z-scan	–	[84]
16	0.017 (solution)	$1.0 \times 10^6$ /TPEF ( $5.3 \times 10^4$ /dimer)	–	[85]
17	$\sim 0.25$ (in toluene) 0.08 (SNPs)	$\sim 7080$ /TPEF	6800	[86]
18	–	TPEF	200,000/particle <sup>a</sup>	[87]
19	0.99 (solution)	128	–	[88]
20	0.05 (solution) 0.16 (NPs)	264/TPEF	–	[40]
<i>Two-dimensional materials</i>				
21	–	1100/Z-scan	–	[89]
22	0.43	2990/TPEF	–	[90]
23	0.86 (solution) 0.56 (NPs)	5300/TPEF	2790	[31]
24	0.25 (NPs)	TPEF	2015 (covered with DSPE-PEG) 2241 (without DSPE-PEG)	[51]
	0.009 (solution) 0.4 (NPs)	8629/Z-scan	–	[91]

(continued)

**Table 2.1** (continued)

Organic Material	Quantum yield ( $\eta$ )	$\sigma_{TPA}$ (solution) GM/technique	$\sigma_{TPA}$ (NPs) GM	Reference
25	0.57	9068/TPEF	–	[92]
26	0.49 (solution) 0.22 (NPs)	25,000/TPEF	9750	[93]
27	–	25,318/Z-scan	–	[94]
28	0.55	11,000/TPEF	–	[95]
29	1 (solution) 0.95 (NPs) 0.75 (SNPs)	9860/TPEF	8481 (NPs) 8686 (SNPs)	[41]
30	–	43,000	–	[83]
31	0.36 (solution)	435/TPEF	87,000	[96]
32	0.48–0.75	$\sim 56,000$ GM/TPEF	–	[97]
33	0.09 (CPNs)	–	11,000/TPEF <sup>a</sup>	[52]
<i>Inorganic materials</i>				
Au (nanorods)	–	–	2320/TPEF <sup>a</sup>	[98]
CdSe-ZnS (QD)	–	–	47,000/TPEF <sup>a</sup>	[99]

These properties correspond to materials in molecular solution and in the form of nanoparticles

<sup>a</sup>In these cases it is reported the two-photon fluorescence excitation cross section  $\sigma_{TPE}$ , namely the product between  $\sigma_{TPA}$  and  $\eta$

(TPM) and photodynamic therapy [24]. For these kind of applications is mandatory that the molecules can show excellent TPA activity in aqueous medium, however, most of them are hydrophobic and those that are soluble in water commonly exhibit low values of  $\sigma_{TPA}$  and  $\eta$  [15, 25, 26]. For instance, water-soluble TPA dyes with  $\sigma_{TPA} \sim 300$  GM have been used as fluorescent markers in biological media [27]. It is important to notate that water not only has a high dielectric constant, which influences the ICT, but it is also capable of producing effective hydrogen bonding and can therefore interact with donor groups in the ground and the excited state [26]. The hydrophobic nature for most of the TPA organic molecules means that organic polar solvents as tetrahydrofuran (THF), dimethylsulfoxide (DMSO), dichloromethane (DCM) or dimethylformamide (DMF) are required to prepare molecular solutions. These and other solvents imply high cytotoxicity. For this reason, a strategy based in the concept of water-dispersible fluorescent organic nanoparticles which are purely composed of hydrophobic molecular aggregates has been studied [28]. This approach works fine, although sometimes promotes aggregation-induced quenching (AIQ) and severe reduction of fluorescence intensity is detected (see Table 2.1). Recently, a new category of TPA fluorescent dyes with exactly the opposite characteristic to the AIQ, aggregation-induced emission (AIE), has been developed [29]. In this context an excellent option is to develop

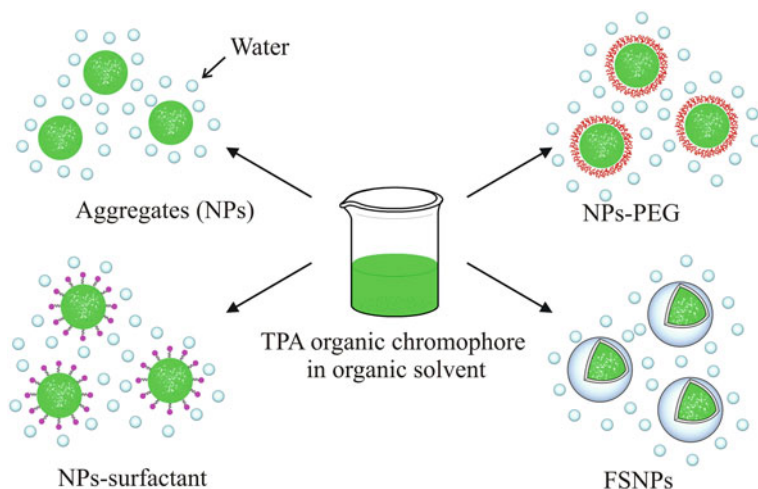


**Fig. 2.8** Scheme of different methods to fabricate nanostructures from TPA chromophores

active TPA materials with high  $\sigma_{TPA}$  and  $\eta$  values such that when they are dispersed in water maintain their optical properties. In this section we will mention some methods that have emerged to incorporate hydrophobic materials into aqueous suspensions. These methods comprise the fabrication of organic nanomaterials in the range from 1 to 100 nm. Figure 2.8 presents schematically different possibilities to generate nanoparticles, i.e., nanoaggregates (NPs), nanoparticles covered by a biocompatible polymer (NPs-PEG) and fluorescent silica nanoparticles (FSNPs).

From the four preparation methods schematized in Fig. 2.8, the reprecipitation technique is the most facile and commonly used to assist the formation of NPs in aqueous media. Reprecipitation method induces the formation of nano-size aggregates that can be stabilized with a surfactant agent (CTAB, triton X-100, albumin, SDS, etc.). The use of surfactants not only stabilizes the suspensions but also protects the surfaces of the formed fluorescent NPs. According to experimental results, these NPs tend to conserve the nonlinear properties showed by the corresponding molecules in solution, although in some cases they showed high cytotoxicity [29, 30]. Recently, it has been demonstrated that the hydrophobic TPA material **23** (see Fig. 2.7; Table 2.1) can be nanostructured by the use micelles generated by dispersing an amphiphilic block copolymer, namely poly(methacrylic acid)-*block*-polystyrene (PMAA-*b*-PS), into water. The  $\sigma_{TPA}$  values for **23** in toluene solution is of 5300 GM and after it is processed into nanoparticles still exhibits a large  $\sigma_{TPA}$  (2790 GM) and high  $\eta$  (0.56) [31]. Another polymer used for the fabrication of NPs doped with hydrophobic TPA dyes is the poly(D,L-lactide-*co*-glycolide) which has the advantage of increasing the compatibility with biological environmental conditions [32].

To further reduce the cytotoxicity of NPs and increase their circulation time *in vivo* studied, they can be encapsulated with polyethylene glycol (PEG). PEG is considered an ideal biocompatible polymer with low toxicity and high water solubility. Some attractive TPA chromophores as silole and hexa-*peri*-hexabenzocorone

( $\sim 1000$  GM) have been covered with PEG derivatives to form NPs-PEG with nonlinearities  $\sim 350$  GM [33, 34].

It is important to note that specific inorganic materials, such as calcium phosphate, have been also used as shells of TPA organic materials to reduce the toxicity, protect and improve their transportation in biological medium. In particular, the inherent properties of calcium phosphate accentuate the potential of this system to enclosed low-weight organic TPA dyes. A general method to encapsulate small fluorescent organic molecules in well-disperse calcium phosphate nanoparticles with diameter under 100 nm was reported [35].

The doping of fluorescent TPA materials (inorganic and organic) into silica NPs is also well-established in the literature. The fabrication of these fluorescent silica nanoparticles (FSNPs) is performed by using a microemulsion method. The advantages of FSNPs are their optical transparency, nonantigenicity, and rich surface chemistry for facile bioconjugation. The silica shell protects the dyes from photobleaching and prevents their interaction with the biological environment. The absorption and emission of the nanoparticles are determined by the properties of encapsulated fluorophores. One of the major disadvantages of using this type of nanoparticles is the phenomenon of aggregation induced fluorescence quenching of the loaded materials [36]. Organic chromophores can also be covalently encapsulated in silica nanoparticles. As an example of this, we can mention the photosensitizer **3** whose TPA properties were retained in the FSNPs, with approximately 1000 GM per unit [37, 38], although the total value per nanoparticle was estimated to be of the order of  $8 \times 10^6$  GM. The TPA dye 9,10-bis[4'-(4''-aminostyryl)styryl]anthracene derivative (**1**) reported by Sehoon Kim et al., showed AIE in the aggregated state. The value of TPA cross-section of **1** in the aggregated state is 217 GM at 775 nm. This TPA dye was used to fabricate organically modified silica (ORMOSIL) nanoparticles with diameter  $< 30$  nm [39].

Our group has oriented investigations in the development of fluorescent TPA chromophores (small organic molecules, dendrimers and polymers) for the fabrication of NPs, NPs-PEG and FSNPs. For instance, we demonstrated that TPA properties of dye **4** ( $\eta = 0.87$ ,  $\sigma_{TPA} = 1000$  GM in THF) with architecture D-A-D is reduced with solvent polarity and hydrogen bonding. However, the formation of aggregates improves the photostability and tends to retain the third-order nonlinear properties ( $\eta = 0.83$ ,  $\sigma_{TPA} = 514$  GM in water) [30]. In addition, typical fluorescent chromophores as BODIPYs have been encapsulated with PEG polymers for bio-imaging applications, see for instance **20** [40]. Similarly, the polymer **29** was investigated in organic solvents and in the form of aggregated and encapsulated structures. In this case, such a polymer showed excellent optical properties, i.e.,  $\sigma_{TPA} = 9860$  GM and  $\eta = 1$  in THF. When the polymer was processed into NP by using the reprecipitation method with CTAB as surfactant, the values of these optical parameters were  $\sigma_{TPA} = 8481$  GM and  $\eta = 0.95$ . Further, for FSNPs fabricated by microemulsion technique the two-photon activity remained similar:  $\eta = 0.75$ ,  $\sigma_{TPA} = 8686$  GM. In addition, the photostability of **29** increased from THF solutions to silica nanoparticles comprising also high cell viability. With the use of this polymer we exemplified that it is possible to process polymers into

nanostructures such that their TPA activity is conserved while simultaneously the requirements for biomedical applications are satisfied. These advantageous characteristics of polymer **29** were used to implement it as sensitive fluorescent contrast agent in TPM for the imaging of lung cancer cell line (A549) and human cervical cancer cell line (HeLa cells), as it is presented in Sect. 2.5 [41]. Thus, for TPM application is important that organic molecules maintain their TPA effect when they are processed into nanostructures. Other examples of organic molecules that tend to maintain their TPA activity are the molecules **1**, **3** and **17** (see Table 2.1). Contrary to this examples, other molecules exhibit detriment of such nonlinear optical property, see for instance the cases of **4**, **23** and **26**.

## 2.5 Biological Applications of TPA Organic Molecules

For organic NPs there are several scientific applications in biomedicine [42]. In this section we briefly describe those associated with TPA properties: two-photon laser scanning microscopy and photodynamic therapy.

### 2.5.1 *Two-Photon Microscopy (TPM)*

Fluorescent microcopy is one of the most versatile techniques in biomedical research. TPM is a three-dimensional imaging technology that was first demonstrated by Denk et al. [1] and is based on the detection of the fluorescence induced by TPA in biomedical samples. For instance, several biological systems often possess endogenous fluorophores, proteins such as tryptophan, tyrosine, phycoerythrin and green fluorescent protein (GFP), neurotransmitter serotonin, coenzyme nicotinamide adenine dinucleotide phosphate [NAD(P)H], etc., such that they represent the source of fluorescence. Exogenous fluorophores can be also artificially added to the biological system under study to enhance the level of signal. The fluorescence produced either by exogenous or endogenous agents provides a direct mechanism for the visualization of cells or subcellular structures, tissue, biological processes and clinical imaging. It should be noted, however, that exogenous fluorophores can surpass in various orders of magnitude the TPA activity of endogenous ones.

To implement TPM a focused laser beam of long wavelength is used to scan the sample under study. In most of the cases the biological sample is stained with an exogenous fluorophores. The excitation is absorbed by the sample via the TPA exhibited by a fluorophore and the emitted fluorescence is collected to create an image point a point of the sample. TPM offers a number of unique advantages, such as reduced specimen photodamage, excitation at low energies (typically infra-red wavelengths) with emission in the visible, enhanced penetration depth, three-dimensional localization of the excitation volume, and high signal-to-background ratio fluorescence

detection [43]. Some of these advantages are consequence of the fact that being the TPA a nonlinear optical process, the magnitude of the induced absorption is intensity dependent so that it can be strongly confined to small volume of excitation within a femtoliter size. In practice, reduced volume of excitation is achieved by tightly focusing laser beams using powerful microscope objectives. Note that optical microscopy based in fluorescence induced by one photon excitation is not able to provide such small volumes of excitation as such absorption is not intensity dependent. Currently, one of the principal motivations in the field of fluorescence microscopy is the development of novel active materials with enhanced TPA properties in order to use them as exogenous fluorophores. These are also known as contrast agents or bio-markers.

The first TPA dyes studied in 1972 [44] were the Rhodamine derivatives which have  $\sigma_{TPA}$  values of 65 (Rhodamine 6G) and 140 GM (Rhodamine B) in methanol solution at the wavelength range 798–802 nm. Later a series of typical one-photon fluorophores (alexa, fluorescein, rhodamines and others) [45, 46] were also investigated for their TPA properties in water or other solvents compatible with biological medium.

Table 2.2 summarizes the optical properties of commercially available TPA dyes [46, 47]. Note that the commercially available dyes in Table 2.2 have rather weak optical properties compared with those novel dyes displayed in Table 2.1.

As mentioned previously (Sect. 2.3), recent investigations have produced a large variety of molecules with  $\sigma_{TPA} > 1000$  GM. The optimization of the nonlinear properties of organic molecules has two central motivations: (a) the reduction of the laser excitation intensity required for imaging (less photodamage) and consequently (b) the opportunity of using less expensive laser systems. On the other hand, various processing methods are being implemented to give to these molecular systems advantages and viability for bio-applications [48]. Here some examples for TPA dyes in the form of NPs, NPs-PEG and FSNPs are presented when they are utilized in TPM to obtain bio imaging of several cell lines. In all cases, the searched features of TPA fluorescence-based contrast agents for TPM are: (a) high quantum yield and high two-photon absorption; (b) adequate dispersibility in the biological environment; (c) non-toxicity; (d) resistance to photobleaching; (e) in vitro and in vivo stability. For comparison purposes, some inorganic materials are also presented as reference.

Photoswitchable fluorescent NPs were fabricated and their surface was bio-conjugated with anti-Her2 antibody, these NPs were employed to analyze the human breast cancer cell line (SK-BR-3) by TPM [49]. Polymers have been employed to protect and stabilized NPs to generate contrast agents. NPs fabricated from a fluorescent resonance energy transfer (FRET) pair, the known hexaphenylsilole and TPA dye **1** inside the micelle of amphiphilic block copolymers poly (methacrylic acid)-*b*-poly(styrene) (PMAA-*b*-PS), were employed to obtain high-quality fluorescent images of RAW cells [34]. Some biopolymers were used to protect NPs, in this context derivatives from PEG are the most employed. BODIPY **19** in NPs-PEG was used as red emissive contrast agent to obtain images of MCF-7 breast cancer cell [40]. Organic TPA dye (2-ter-butyl-0,10-di(naphthalene-2-yl) anthracene (TBADN) was employed to fabricate NPs in which the surface was modified with the surfactant poly(maleic anhydride-alt-1-octadecene)-polyethylene

**Table 2.2** TPA activity for commercial fluorophores in water

Dyes	Wavelength (nm)	$\eta \times \sigma_{TPA}$ (GM)
Alexa350	700	35
Alexa480	750	100
Alexa568	780	180
Alexa594	780	100
Bodipy	930	18
Ca-Crimson	870	100
Ca-Green	950	60
Cascade blue	740	2.5
Coumarine307 <sup>a</sup>	800	15
DAPI	700	100
Di-4-ANEPPS <sup>b</sup>	950	5
Di-8-ANEPPS <sup>b</sup>	950	10
Dil <sup>a</sup>	700	95
dsRed	1000	110
eGFP	930	180
Fluorescein	780	38
Fluo-3	800	13
Riboflavina	700	1
Retinol	700	0.1
Folic acid	700	0.01
Lucifer yellow	850	1.4
mCerulean	850	78
mCFP	850	190
NADH in PBS	700	0.09

<sup>a</sup>Tested in methanol<sup>b</sup>Tested in ethanol

glycol (C18PMH-PEG) and then bioconjugated with folic acid, bioimaging showed a selectivity for KB cell [50]. Folic acid-functionalized NPs-PEG of TPA chromophore **24** were used for targeting MCF-7 cancer cell by TPM technique [51]. Conjugated polymers are also attractive candidates to address the requirements for TPM imaging. NPs from conjugated polymer poly(p-phenylene ethylene) (**33**) were prepared by ultrafiltration technique. Average size for these NPs was of 8 nm and with a  $\sigma_{TPA}$  of 11,000 GM at 730 nm. The hydrophilicity and nontoxicity of **33**-NPs were employed to obtain several bio-images of endothelial cell by TPM [52]. In the case of inorganic materials with excellent luminescence and nonlinear properties, there are many examples of how NPs have been also applied as contrast agents in TPM. For instance, bio-conjugated QDs (CdSe/CdS/ZnS) with anti-caludin-4 were reported as optical contrast agent for imaging pancreatic cell in vitro using transferrin as targeting biomolecule [53]. In another example, aqueous dispersable NaYF<sub>4</sub> nanocrystals of 20–30 nm coped with RE ions Tm<sup>3+</sup> and Yb<sup>3+</sup> (UCNPs) were applied for in vitro TPM imaging, while the red emission ( $\sim 800$  nm) of UCNPs was used for obtain the imaging of pancreatic cancer cell, no apparent



cytotoxicity was observed [54]. Many other examples of inorganic nanoparticles employed for bio-imaging can be found in the literature [27].

Fluorescent SNPs have received strong interest in various cancer imaging applications [55–57]. FSNPs loaded with 25 % of TPA chromophore **1** (~2500 molecules per nanoparticles) were used as efficient probes for TPM with extraordinary signal output, without any sign of cytotoxicity in HeLa cell [58]. FSNPs doped with TPA dye **2** were fabricated and the surface bioconjugated with folic acid; these FSNPs were employed to study in vitro the selectivity for HeLa cell cancer by TPM [59]. To increase the stability of FSNPs for in vivo imaging PEG derivatives are often introduced to their surface (FSNP-PEG). FSNPs-PEG doped with derivative 2-(2,6-bis((E)-2-(7-(diphenylamino)-9,9-diethyl-9Hfluoren-2-yl)vinyl)-4H-pyran-4-ylidene) malononitrile (DFP) bioconjugated with folic acid derivative have been employed to mark HeLa cells due to folate receptor interaction for in vivo analysis [60]. Of course, the use of SNPs loaded with inorganic materials has been also extensively reported in the literature. For instance, SNPs doped with Gold NPs were fabricated, these materials glow brightly when are excited by near-infrared light exhibiting  $\sigma_{TPA}$  of 2300 GM, which demonstrate the potential application to obtain biological imaging in bulk by two-photon-induced photoluminescence [61]. QDs and magnetic ( $\text{Fe}_3\text{O}_4$ ) were co-encapsulated within SNPs and their surface was bioconjugated with transferrin, the magnetic properties of these SNPs were used in vitro to guide into Human pancreatic carcinoma (Panc-1) line cell line and optical for obtain TPF-bioimaging [62].

Our group has fabricated NPs, NPs-PEG and FSNPs from organic dyes and polymers. One of our major interests is to study how nonlinearities can be conserved or changed as these TPA materials are processed into nano-structured systems intended to be used as contrast agents in TPM. Some of our results were presented in Sect. 2.4 regarding the conjugated polymer **29**, and it was discussed that this polymer tend to conserve its TPA action in the form of NPs, NPs-PEG and FSNPs as compared with that exhibited in molecular solution [41]. Taking advantage of this characteristic of our organic nanoparticles, the imaging of human cervical cancer cell line (HeLa cell) was performed. Figure 2.9 presents images from fluorescence microscopy obtained using the polymer **29** as contrast agent excited with either one-photon (488 nm) or two-photons (740 nm), showing the equivalence of the so obtained images, but in the latter case the use of infrared wavelengths is advantageous in the terms of less photodamage provoked (less invasive) to the biological specimen. For comparison purposes, we also present the images obtained for the same cellular line stained with the corresponding monomer of **29** (denoted as **M29**). **M29** and **29** were processed as NPs by precipitation technique and stabilized with surfactant (CTAB). These NPs showed large fluorescence and high photostability compared with the data collected in solution. The TPEF experiments for NPs of **M29** showed values of  $\eta \sim 1$  and  $\sigma_{TPA}$  of 72 GM, while for NPs of **29** a higher value of  $\sigma_{TPA}$  (8481 GM) was obtained with  $\eta = 0.95$ . According to the images presented in Fig. 2.9, similar results are obtained with the use of **M29** or **29**. Nevertheless, the use of big molecules (polymers, hyperbranched polymers, dendrimers) as contrast agents is attractive because in

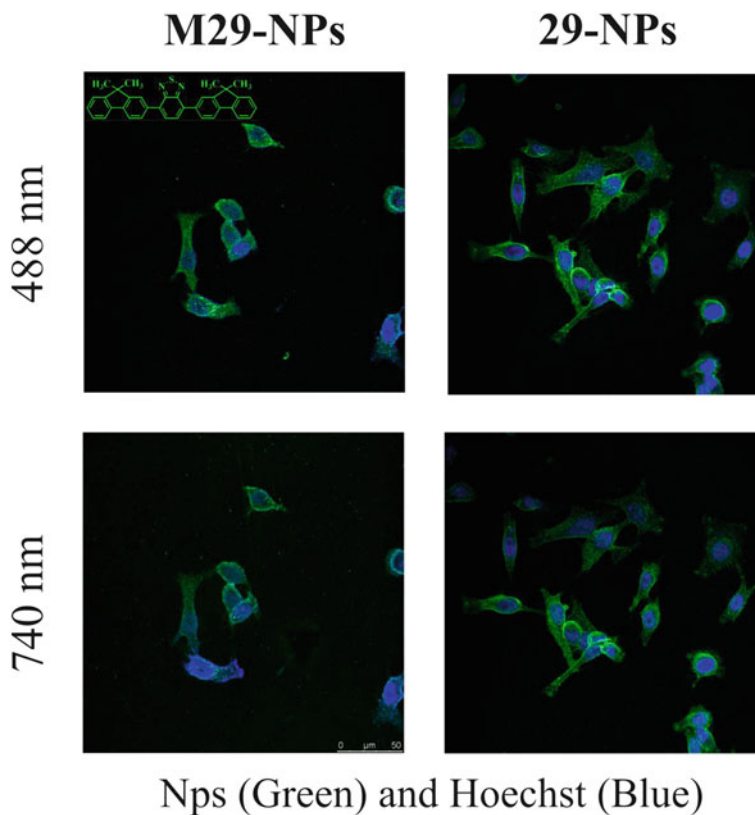


**Fig. 2.9** One-photon (*first row*) and two-photon (*second row*) fluorescence images of HeLa cells treated with NPs of the monomer **M29** (*first column*) and the corresponding polymer **29** (*second column*). The excitation wavelengths are indicated to the *left of the columns*. The NPs penetrated nonspecifically into the cell and remained in the cytoplasm (*green emission*). The dye Hoechst 33258 was used to specifically stain the nucleus cell (*blue emission*). The fluorescence of this dye was obtained in all cases with one-photon excitation and the so obtained image merged to that corresponding to the two-photon excitation. The chemical structure of **M29** is shown in the picture of the first row and first column. The chemical structure of **29** is presented in Fig. 2.7

many cases they exhibit enhanced nonlinearities (per repeated unit of the polymer chain) in comparison to small organic molecules. Further, in our work it was demonstrated that it is possible to fabricate FSNPs with the polymer **29** to be used as contrast agents in TPM [41]. Notice that most of the attention given to FSNP in the literature is related to small organic molecules.

### 2.5.1.1 Photodynamic Therapy

Photodynamic therapy (PDT) has emerged as an alternative non-invasive and selective tool for blood purification and to destroy small cancerous tumors [8, 37, 63], i.e., for the

treatment of superficial tumors in oesophagus, bladder and melanoma cancer [64]. This technique involves the use of a photosensitizer (PS) which, upon irradiation at specific wavelengths in the presence of oxygen, leads to the generation of cytotoxic species (singlet oxygen  $^1\text{O}_2$ ) and consequently to irreversible cell damage (Fig. 2.10). Usually, conventional photosensitizers (porfimer sodium Photofrin<sup>®</sup>, 5-aminovulnic acid ALA-Levulan<sup>®</sup>, verteporfin Visudyne<sup>®</sup> and methyl ester of ALA Metvix<sup>®</sup>) require very high intensity of excitation [65] (close to the threshold of tissue photodamage) at visible wavelengths. PDT combined with two-photon absorption in the near-IR region can circumvent this limitation. This approach offers new perspectives for the treatment of tumors providing a technique which is less invasive since the photodynamic effect can be limited to the area of interest, leaving the surrounding healthy tissues and cells undamaged. This is because, as it was discussed previously, the TPA is a process that depends on the intensity of excitation, and such a process only takes place when laser pulses are strongly focused in small volumes. Nevertheless, a bottle neck to make practical this application via TPA is that the commercially available PSs have weak two-photon absorption cross sections. Thus, there is an opportunity to develop new PS materials with a high TPA response in the biomedical window (650–1000 nm).

Recently novel organic materials and nanostructures have been tested as interesting supplies for PDT by using TPA properties [63]; some water soluble polymers [66], aggregated species [67] and modified silica nanoparticles [68] have been studied. In this respect, colloidal carriers for PSs, such as oil-dispersion, liposomes, low-density lipoproteins, polymeric micelles and silica nanoparticles, offer advantages as cell permeability and retention effect and active targeting by using surface modification. There are two main approaches for optimization of NPs systems for

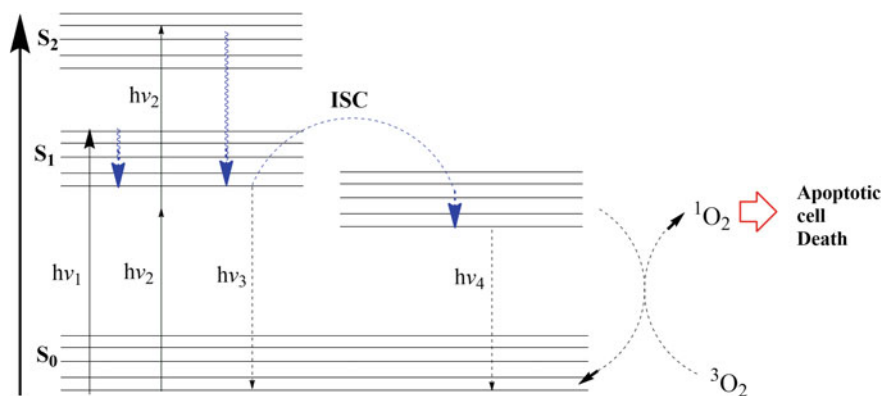


**Fig. 2.10** Jablonski diagram depicting the photophysical processes for one-photon excitation and two-photon excitation of PDT. Excitation state of organic dyes is obtained by absorption of one or two photon (pulsed laser light). After excitation in either case, the molecule relaxes to the lowest vibrational level of the first singlet excited state. From here, it can emit photon (fluorescence) or undergo intersystem crossing (ISC) into the first triplet state. From the triplet state, this can emit phosphoresce or nonradiatively transfer its energy to convert the molecular oxygen  $^3\text{O}_2$  to the cytotoxic singlet oxygen  $^1\text{O}_2$ . Singlet oxygen can then activate the apoptotic cell death pathway

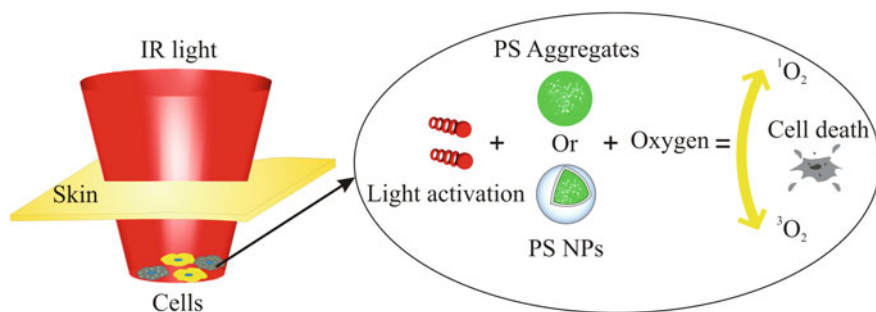


**Fig. 2.11** Representation of organic nanomaterials with TPA properties employed in PDT. Infrared light activates nanoparticles (PS aggregates or NPs loaded with PS) through the absorption of two-photons. After sensitization the PS produces cytotoxic species (singlet oxygen  $^1O_2$ ) able to produce cell damage

PDT (Fig. 2.11): (i) design of new photosensitizers or chemical modification of the existing ones to produce efficient sensitization through TPA process, (ii) employ the energy-transfer process from efficient TPA toward typical PS. For the latter, the PS (energy acceptor) is indirectly excited through fluorescent resonance energy transfer (FRET) from the TPA dye (energy donor) [69–71]. In general, commercial PS used in PDT as Verteporfin, Photofrin<sup>®</sup> and protoporphyrin IX (PpIX) have very low  $\sigma_{TPA}$  value, in this case 31, 7.5 and 10 GM, respectively [63, 72]. To increase their activity (cytotoxicity induced by the singlet oxygen generation) at infrared wavelengths they are encapsulate in SNPs with some efficient TPA dye (energy donor) [73]. As examples of this approach, we can mention the PDT employing SNPs doped with no commercial TPA dye **3** and bioconjugated with mannose to treat retinoblastoma cancer cells (Y-79) [74] or SNPs loaded with PpIX to treat HeLa cells [75].

**Acknowledgements** G. Ramos-Ortiz thanks financial support from the National Mexican Agency for Science and Technology (Conacyt).

## References

1. W. Denk, J.H. Strickler, W.W. Webb, Two-photon laser scanning fluorescent microscopy. *Science* **248**(6), 73–76 (1990)
2. H.H. Fang, Q.D. Chen, J. Yang, H. Xia, Y.-G. Ma, H.-Y. Wang, H.-B. Sun, Two-photon excited highly polarized and directional upconversion emission from slab organic crystals. *Opt. Lett.* **35**(3), 441–443 (2010)
3. H. Guang, Y. Lixiang, P.N. Prasad, A. Abboto, A. Facchetti, G.A. Pagani, Two-photon pumped frequency-upconversion lasing of a new blue-green dye material. *Opt. Commun.* **140** (1–3), 49–52 (1997)

4. J.E. Ehrlich, X.L. Wu, I.-Y.S. Lee, Z.-Y. Hu, H. Röckel, S.R. Marder, J.W. Perry, Two-photon absorption and broadband optical limiting with bis-donor stilbenes. *Opt. Lett.* **22**(24), 1843–1845 (1997)
5. P. Wei, O.F. Tan, Y. Zhu, G.H. Duan, Axial superresolution of two-photon microfabrication. *Appl. Opt.* **46**(18), 3694–3699 (2007)
6. N.S. Makarov, A. Rebane, M. Drobizhev, H. Wolleb, H. Spahn, Optimization two-photon absorption for volumetric storage. *J. Opt. Soc. Am. B* **24**(8), 1874–1885 (2007)
7. S.J. Pond, O. Tsutsumi, M. Rumi, O. Kwon, E. Zojer, J.L. Brédas, S.R. Marder, J.W. Perry, Metal-ion sensing fluorophores with large two-photon absorption cross sections: Aza-crown ether substituted donor-acceptor-donor distyrylbenzenes. Development of highly fluorescent silica nanoparticles chemically doped with organic dye for sensitive DNA microarray detection. *J Am Chem Soc.* **126**(30), 9291–9306 (2004)
8. S. Kim, T.Y. Ohulchanskyy, H.E. Pudavar, R.K. Pandey, P.N. Prasad, Organically modified silica nanoparticles co-encapsulating photosensitizing drugs and aggregation-enhanced two-photon absorbing fluorescent dye aggregates for two photon therapy. *J. Am. Chem. Soc.* **129**(9), 2669–2675 (2007)
9. M. Khurana, H.A. Collins, A. Karotki, H.L. Anderson, D.T. Cramb, B.C. Wilson, Quantitative *in vitro* demonstration of two-photon photodynamic therapy using photofrin and visudyne. *Photochem. Photobio.* **83**(6), 1441–1448 (2007)
10. M. Göppert-Mayer, Über Elementarakte mit zwei Quantensprüngen. *Ann. Phys. (Leipzig)* **9**, 273 (1931)
11. M.C. Rumi, J.W. Perry, Two-photon absorption: an overview of measurements and principles. *Adv. Opt. Photon.* **2**(4), 451–518 (2010)
12. M. Sheik-Bahae, A.A. Said, T.H. Wei, D.J. Hagan, E.W. Van Stryland, Sensitive measurement of optical nonlinearities using a single beam. *IEEE LEOS NEWSLETTER* **21** (1), 17–26 (2007). (Special 30th Anniversary Feature)
13. L. Antonov, K. Kamada, K. Ohta, Estimation of two-photon absorption characteristic by a global fitting procedure. *Appl. Spectrosc.* **56**(11), 1508–1511 (2002)
14. K. Kamada, K. Ohta, Y. Iwase, K. Kondo, Two-photon absorption properties of symmetric substituted diacetylene: drastic enhanced of the cross section near the one-photon absorption peak. *Chem. Phys. Lett.* **372**(3–4), 386–393 (2003)
15. C. Xu, W.W. Webb, Measurement of two-photon excitation cross section of molecular fluorophores with data from 690 to 1050 nm. *J. Opt. Soc. Am. B* **13**(3), 481–491 (1996)
16. A. Taouri, H. Derbal, J.M. Nunzi, R. Mountasser, M. Sylla, Two-photon absorption cross-section measurement by thermal lens and nonlinear transmission methods in organic materials at 532 and 1064 nm laser excitation. *J. Optoelectronic Adv. Mater.* **11**(11), 1696–1703 (2009)
17. C.V. Bindhu, S.S. Harilal, V.P.N. Nampoori, C.P.G. Vallabhan, Investigation of nonlinear absorption and aggregation in aqueous solution of rhodamine B using thermal lens technique. *PRAMANA-J. Phys.* **52**(4), 435–442 (1999)
18. C.V. Bindhu, S.S. Harilal, R.C. Issac, G.K. Varier, V.P.N. Nampoori, C.P.G. Vallabhan, Pulsed photoacoustic technique to study nonlinear processes in liquids: results in toluene. *PRAMANA-J. Phys.* **44**(3), 231–235 (1995)
19. M.A. Albota, C. Xu, W.W. Webb, Two-photon fluorescence excitation cross section of biomolecular probes from 690 to 960 nm. *App. Opt.* **37**(31), 7352–7356 (1998)
20. G.S. He, L.-S. Tan, Q. Zheng, P.N. Prasad, Multiphoton absorbing materials: molecular design, characterizations and applications. *Chem. Rev.* **108**(4), 1245–1330 (2008)
21. M. Pawlicki, H.A. Collins, R.G. Denning, H.L. Anderson, Two-photon absorption and the design of two-photon dyes. *Angew. Chem. Int. Ed.* **48**(18), 3244–3266 (2009)
22. M. Rumi, J.E. Ehrlich, A.A. Heikal, J.W. Perry, S. Barlow, Z. Hu, D. McCord-Maughon, T.C. Parker, H. Röckel, S. Thayumanavan, S.R. Marder, D. Beljonne, J.-L. Brédas, Structure-property relationship for two-photon absorbing chromophores: bis-donor diphenylpolyene and bis(styrylbenzene derivatives). *J. Am. Chem. Soc.* **122**(39), 9500–9510 (2000)

23. B.A. Reinhardt, L.L. Brott, S.J. Clarson, A.G. Dillard, J.C. Bhatt, R. Kannan, L. Yuan, G.S. He, P.N. Prasad, Highly active two-photon dyes: design, synthesis, and characterization toward application. *Chem. Mater.* **10**(7), 1863–1874 (1998)
24. H.M. Kim, B.R. Cho, Two-photon materials with large two photon cross section. Structure property relationship. *Chem. Commun.* **2**, 153–164 (2009)
25. F. Nicoud, F. Bolze, X.-H. Sun, A. Hayek, P. Baldeck, Boron-containing two-photon absorbing chromophores. 3(1) one- and two-photon photophysical properties of *p*-carborane-containing fluorescent bioprobes. *Inorg. Chem.* **50**(10), 4272–4278 (2011)
26. H.Y. Woo, B. Liu, B. Kholer, D. Korystov, A. Mikhailovsky, G.C. Bazan, Solvent effects on the two-photon absorption of distyrylbenzene chromophores. *J. Am. Chem. Soc.* **127**(42), 14721–14729 (2005)
27. P. Sharma, S. Brown, G. Walter, S. Santra, B. Moudgil, Nanoparticles for bioimaging. *Adv. Colloid Interface Sci.* **123–126**, 471–485 (2006)
28. H. Kasai, H.S. Nalwa, H. Oikawa, S. Okada, H. Matsuda, N. Minami, A. Kakuta, K. Ono, A. Mukoh, H. Nakanishi, A novel preparation method of organic microcrystals. *Jpn. J. Appl. Phys* **31**, L1132 (1992)
29. S. Kim, Q. Zheng, G.S. He, D.J. Bharali, H.E. Pudavar, A. Baev, P.N. Prasad, Aggregation-enhanced fluorescence and two-photon absorption in nanoaggregates of a 9,10-bis[4'-(4''-aminostyryl)styryl]anthracene derivative. *Adv. Funct. Mater.* **16**, 2317–2323 (2006)
30. J. Rodríguez-Romero, L. Aparicio-Ixta, M. Rodríguez, G. Ramos-Ortiz, J.L. Maldonado, A. Jiménez-Sánchez, N. Farfán, R. Santillan, Synthesis, chemical-optical characterization and solvent interaction effect of novel fluorene-chromophores with D-A-D structure. *Dyes Pigm.* **98**(1), 31–41 (2013)
31. Y. Tian, C.-Y. Chen, Y.-J. Cheng, A.C. Young, N.M. Tucker, A.K.-Y. Jen, Hydrophobic chromophores in aqueous micellar solution showing large two-photon absorption cross sections. *Adv. Funct. Mater.* **17**(10), 1691–1697 (2007)
32. K. Baba, T.Y. Ohulchanskyy, Q. Zheng, T.C. Lin, E.J. Bergey, P.N. Prasad, Infrared emitting dye and/or two photon excitable fluorescent dye encapsulated in biodegradable polymer nanoparticles for bioimaging. *Mater. Res. Soc. Symp. Proc.* **845**, 209–214 (2005)
33. Q. Zheng, T.Y. Ohulchanskyy, Y. Sahoo, P.N. Prasad, Water-dispersible polymeric structure co-encapsulation a novel hexa-peri-hexabenzocoronene core containing chromophore with enhanced two-photon absorption an magnetic nanoparticles for magnetically guided two-photon cellular imaging. *J. Phys. Chem. C* **111**(45), 16846–16851 (2007)
34. W.-C. Wu, C.-Y. Chen, Y. Tian, S.-H. Jang, Y. Hong, Y. Liu, R. Hu, B.Z. Tang, Y.-T. Lee, C.-T. Chen, W.-C. Chen, A.K.-Y. Jen, Enhancement of aggregation-induced emission in dye-encapsulating polymeric micelles for bioimaging. *Adv. Funct. Mater.* **20**, 1413–1423 (2010)
35. T.T. Morgan, H.S. Muddana, Eİ. Altinođ, S.M. Rouse, A. Tabaković, T. Tabouillot, T. J. Russin, S.S. Shanmugavelandy, P.J. Butler, P.C. Eklund, J.K. Yun, M. Kester, J.H. Adair, Encapsulation of organic molecules in calcium phosphate nanocomposite particles for intracellular imaging and drug delivery. *NanoLett.* **8**(12), 4108–4115 (2008)
36. T.Y. Ohulchanskyy, I. Roy, K.-T. Yong, H.E. Pudavar, P.N. Prasad, High-resolution light microscopy using luminescent nanoparticles. *WIREs Nanomed. Nanobiotechnol.* **2**(2), 162–175 (2010)
37. M. Gary-Bobo, Y. Mir, C. Rouxel, D. Brevet, I. Basile, M. Maynadier, O. Vaillant, O. Mongin, M. Blanchard-Desce, A. Morère, M. Garcia, J.-O. Durand, L. Raehm, Mannose-functionalized mesoporous silica nanoparticles for efficient two-photon photodynamic therapy of solid tumors. *Angew. Chem.* **123**(48), 11627–11631 (2011)
38. C. Rouxel, M. Charlot, Y. Mir, C. Frochot, O. Mongin, M. Blanchard-Desce, Banana-shaped biophotonics quadrupolar chromophores: from fluorophores to biophotonic photosensitizers. *New J. Chem.* **35**, 1771–1780 (2011)

39. S. Kim, H.E. Pudavar, A. Bonoiu, P.N. Prasad, Aggregation-enhanced fluorescence in organically modified silica nanoparticles: a novel approach toward high-signal-output nanoprobe for two-photon fluorescence bioimaging. *Adv. Mater.* **19**(22), 3791–3795 (2007)
40. Z. Zhao, B. Chen, J. Geng, Z. Chang, L. Aparicio-Ixta, H. Nie, C.C. Goh, L.G. Ng, A. Qin, G. Ramos-Ortiz, B. Liu, B. Zhong, Red emissive biocompatible nanoparticles from tetraphenylethene-decorated BODIPY luminogens for two-photon excited fluorescence cellular imaging and mouse brain blood vascular visualization. *Part. Part. Syst. Charact.* **31**(4), 481–491 (2014)
41. L. Aparicio-Ixta, G. Ramos-Ortiz, J.L. Pichardo-Molina, J.L. Maldonado, M. Rodríguez, V.M. Tellez-Lopez, D. Martinez-Fong, M.G. Zolotukhin, S. Fomine, M.A. Meneses-Nava, O. Barbosa-García, Two-photon excited fluorescence of silica nanoparticles loaded with a fluorene-based monomer and its cross-conjugated polymer: their application to cell imaging. *Nanoscale* **4**, 7751–7759 (2012)
42. S. Krol, R. Macrez, F. Docagne, G. Defer, S. Laurent, M. Rahman, M.J. Hajipour, P. Kehoe, M. Mahmoudi, Therapeutic benefits from nanoparticles: the potential significance of nanoscience in diseases with compromise to the blood brain barrier. *Chem. Rev.* **113**(3), 1877–1903 (2013)
43. P.T.C. So, C.Y. Dong, B.R. Masters, K.M. Berland, Two-photon excitation fluorescence microscopy. *Annu. Rev. Biomed. Eng.* **2**, 399–429 (2000)
44. P. Hermann, J. Ducuing, Dispersion of the two-photon cross section in rhodamine dyes. *Opt. Commun.* **6**(2), 101–105 (1972)
45. N.S. Makarov, M. Drobizhev, A. Rebane, Two-photon absorption standards in the 550–1600 nm excitation wavelength range. *Opt. Express* **16**(6), 4029–4047 (2008)
46. J.R. Lakowicz, *Principles of Fluorescence Spectroscopy*, 3rd edn. (Springer, Berlin, 2010). 2010
47. K. Svoboda, R. Yasuda, Principles of two-photon excitation microscopy and its applications to neuroscience. *Neuron* **50**, 823–839 (2006)
48. S.S. Agasti, S. Rana, M.-H. Park, C. Kim, C.-C. You, V. Rotello, Nanoparticles for detection and diagnostic. *Adv. Drug Delivery Rev.* **62**(3), 316–328 (2010)
49. M.-Q. Zhu, G.-F. Zhang, C. Li, M. Aldred, E. Chang, R. Drezek, A.D.Q. Li, Reversible two-photon photoswitching and two-photon imaging of immunofunctionalized nanoparticles target to cancer cells. *J. Am. Chem. Soc.* **133**(2), 365–372 (2011)
50. X. Diao, W. Li, J. Yu, X. Wang, X. Zhang, Y. Yang, F. An, Z. Liu, X. Zhang, Carrier-free, water dispersible and highly luminescent dye nanoparticles for targeted cell imaging. *Nanoscale* **4**, 5373–5377 (2012)
51. K. Li, Y. Jiang, D. Ding, X. Zhang, Y. Liu, J. Hua, S.S. Feng, B. Liu, Folic acid-functionalized two-photon absorbing nanoparticles for targeted MCF-7 cancer cell imaging. *Chem. Commun.* **47**, 7323–7325 (2011)
52. N.A. Abdul, W. McDaniel, K. Bardon, S. Srinivasan, V. Vickerman, P.T.C. So, J. Ho, Conjugated polymer nanoparticles for two-photon imaging of endothelial cells in a tissue model. *Adv. Mater.* **21**, 3492–3496 (2009)
53. J. QianYao, K.-T. Yong, I. Roy, T.Y. Ohulchanskyy, E.J. Bergey, Imaging pancreatic cancer using surface-functionalized quantum dots. *J. Phys. Chem. B* **111**, 6969–6972 (2007)
54. M. Nyk, R. Kumar, T.Y. Ohulchanskyy, E.J. Bergey, P.N. Prasad, High contrast in vitro and in vivo photoluminescence bioimaging using near infrared to near infrared up-conversion in TM3+ and Yb3+ doped fluoride nanophosphors. *NanoLett.* **8**, 3834–3838 (2008)
55. S. Santra, P. Zhang, K.M. Wang, R. Tapeç, W.H. Tan, Conjugation of biomolecules with luminophore-doped silica nanoparticles for photostable biomarkers. *Anal. Chem.* **73**, 4988–4993 (2001)
56. J.E. Smith, C.D. Medley, Z.W. Tang, D. Shangguan, C. Lofton, W.H. Tan, Aptamer-conjugated nanoparticles for the collection and detection of multiple cancer cells. *Anal. Chem.* **79**, 3075–3082 (2007)
57. G. Yao, L. Wang, Y.R. Wu, J. Smith, J.S. Xu, W.J. Zhao, E.J. Lee, W.H. Tan, FloDots: luminescent nanoparticles. *Anal. Bioanal. Chem.* **385**, 518–524 (2006)

58. S.H. Kim, H. Huang, H.E. Pudavar, Y.P. Cui, P.N. Prasad, Intraparticle energy transfer and fluorescence photoconversion in nanoparticles: an optical highlighter nanoprobe for two-photon bioimaging. *Chem. Mater.* **19**, 5650–5656 (2007)
59. X. Wang, S. Yao, H.-Y. Ahn, Y. Zhang, M.V. Bondar, J.A. Torres, K.D. Belfield, Folate receptor targeting silica nanoparticles probe for two-photon fluorescence bioimaging. *Biomed. Opt. Express* **1**(2), 453–462 (2010)
60. X. Wang, A.R. Morales, T. Urakami, L. Zhang, M. Bondar, M. Komatsu, K.D. Belfield, Folate receptor-target aggregation-enhanced near-IR emitting silica nanoprobe for one-photon in vivo and two-photon ex vivo fluorescence bioimaging. *Bioconjugate Chem.* **22**(7), 1438–1450 (2011)
61. J. Park, A. Estrada, K. Sharp, K. Sang, J. Schwartz, D. Smith, C. Coleman, J.D. Payne, B.A. Korgel, A. Dunn, J.W. Tunell, Two-photon-induced photoluminescence imaging of tumors using near-infrared excited gold nanoshells. *Opt. Express* **16**(3), 1590–1599 (2008)
62. W.-C. Law, K.-T. Yong, I. Roy, G. Xu, H. Ding, E.J. Bergey, H. Zeng, P.N. Prasad, Optically and magnetically doped modified silica nanoparticles as efficient magnetically guide biomarker for two-photon imaging of live cells. *J. Phys. Chem. C* **112**(21), 7972–7977 (2008)
63. J.P. Celli, B.Q. Spring, I. Rizvi, C.L. Evans, K.S. Samkoe, S. Verma, B.W. Pogue, T. Hasan, Imaging and photodynamic therapy: mechanisms, monitoring and optimization. *Chem. Rev.* **110**(5), 2795–2838 (2010)
64. M. Triesscheijn, P. Baas, J.H.M. Schellens, F. Stewart, Photodynamic therapy in oncology. *Oncologist* **11**, 1034–1044 (2006)
65. N. He, B. Li, H. Zhang, J. Hua, S. Jiang, Synthesis, two-photon absorption and optical limiting properties of new linear and multi-branched bithiazole-based derivatives. *Synth. Met.* **162**, 217–224 (2012)
66. X. Shen, L. Li, A.C.M. Chan, N. Gao, S.Q. Yao, Q.-H. Xu, Water-soluble conjugated polymers for simultaneous Two-photon cell imaging and Two-photon photodynamic therapy. *Adv. Opt. Mater.* **1**, 92–99 (2013)
67. L. Kelbaskas, W. Dietel, Internalization of aggregated photosensitizer by tumor cells: subcellular time-resolved fluorescence spectroscopy on derivatives of pyropheophorbide-a ethers and chlorin e6 under femtosecond one- and two-photon excitation. *Photochem. Photobiol.* **76**(6), 686–694 (2002)
68. S. Kim, T.Y. Ohulchansky, H.E. Pudavar, R.K. Pandey, P.N. Prasad, Organically modified silica nanoparticles coencapsulating photosensitizing drug and aggregation-enhanced two photon absorbing fluorescent dye aggregates for two-photon photodynamic therapy. *J. Am. Chem. Soc.* **129**, 2669–2675 (2007)
69. W.R. Dichtel, J.M. Serin, C. Edler, J.M.J. Fréchet, M. Matuszewski, L.-S. Tang, T.Y. Ohulchansky, P.N. Prasad, Singlet oxygen generation via two-photon excited FRET. *J. Am. Chem. Soc.* **126**(17), 5380–5381 (2004)
70. M.A. Oar, J.M. Serin, W.R. Dichtel, J.M. Fréchet, Photosensitization of singlet oxygen via two-photon-excited fluorescence resonance energy transfer in water-soluble dendrimer. *Chem. Mater.* **17**, 2267–2275 (2005)
71. X. Shen, F. He, J. Wu, G.Q. Xu, S.Q. Yao, Q.-H. Xu, Enhanced two-photon singlet oxygen generation by photosensitizer-doped conjugate polymer nanoparticles. *Langmuir* **27**(5), 1739–1744 (2011)
72. K.S. Samkoe, A.A. Clancy, A. Karotki, B.C. Wilson, D.T. Cramb, Complete blood vessel occlusion in the chick chorioallantoic membrane using two-photon excitation photodynamic therapy: implications for treatment of wet age-related macular degeneration. *J. Biomed. Opt.* **12**(3), 034025-1–034025-14 (2007)
73. S.-H. Cheng, C.-C. Hsieh, N.-T. Chen, C.-H. Chu, C.-M. Huang, P.-T. Chou, F.-G. Tseng, C.-S. Yang, C.-Y. Mou, L.-W. Lo, Well-defined mesoporous nanostructure modulates three-dimensional interface energy transfer for two-photon activated photodynamic therapy. *Nano Today* **6**, 552–563 (2011)
74. M. Gary-Bobo, Y. Mir, C. Rouxel, D. Brevet, O. Hocine, M. Maynadier, A. Gallud, A. Silva, O. Mongin, M. Blanchard-Desce, S. Richeter, B. Looockd, P. Maillard, A. Morère, M. Garcia,



- L. Raehm, J.-O. Durand, Multifunctionalized mesoporous silica nanoparticles for the *in vitro* treatment of retinoblastoma: drug deliver, one and two-photon photodynamic therapy. *Int. J. Pharm.* **432**, 99–104 (2012)
75. J. Qian, D. Wang, F. Cai, Q. Zhan, Y. Wang, S. He, Photosensitizer encapsulated organically modified silica nanoparticles for direct two-photon photodynamic therapy and *in vivo* functional imaging. *Biomaterials* **33**(19), 4851–4860 (2012)
76. C. Huang, C. Lin, A. Ren, N. Yang, Dicyanostilbene-derived two-photon fluorescence dyes with large two-photon absorption cross sections. *J. Mol. Struct.* **1006**(1–3), 91–95 (2011)
77. Y. Tan, Q. Zhang, J. Yu, X. Zhao, Y. Tian, Y. Cui, X. Hao, Y. Yang, G. Qian, Solvent effect on two-photon absorption (TPA) of three novel dyes with large TPA cross-section and red emission. *Dyes Pigm.* **97**(1), 58–64 (2013)
78. D. Xu, Z. Yu, M. Yang, Z. Zheng, L. Zhu, X. Zhang, L. Ye, J. Wu, Y. Tian, H. Zhou, 2,20-Bipyridine derivatives containing aza-crown ether: structure, two-photon absorption and bioimaging. *Dyes Pigm.* **100**, 142–149 (2014)
79. C. Huang, X. Peng, D. Yi, J. Qu, H. Niu, Dicyanostilbene-based two-photon thermo-solvatochromic fluorescence probes with large two-photon absorption cross sections: detection of solvent polarities, viscosities, and temperature. *Sens. Actuators B* **182**, 521–529 (2013)
80. F. Hao, Z. Liu, M. Zhang, J. Liu, S. Zhang, J. Wu, H. Zhou, Y.-P. Tian, Four new two-photon polymerization initiators with varying donor and conjugated bridge: Synthesis and two-photon activity. *Spectrochim. Acta Part A Mol. Biomol. Spectrosc.* **118**, 538–542 (2014)
81. H.A. Collins, M. Khurana, E.H. Moriyama, A. Mariampillai, E. Dahlstedt, M. Balaz, M.K. Kuimova, M. Drobnizhev, V.X.D. Yang, D. Phillips, A. Rebane, B.C. Wilson, H.L. Anderson, Blood-vessel closure using photosensitizers engineered for two-photon excitation. *Nature Photonics* **2**, 420–424 (2008)
82. A.R. Morales, G. Luchita, C.O. Yanez, M.V. Bondar, O.V. Przhonska, K.D. Belfield, Linear and nonlinear photophysics and bioimaging of an integrin-targeting water-soluble fluorenyl probe. *Org. Biomol. Chem.* **8**(11), 2600–2608 (2010)
83. N. Aratani, D. Kim, A. Osuka,  $\pi$ -conjugation enlargement toward the creation of multi-porphyrinic systems with large two-photon absorption properties. *Chem. Asian J.* **4** (8), 1172–1182 (2009)
84. T.K. Ahn, K.S. Kim, D.Y. Kim, S.B. Noh, N. Aratani, C. Ikeda, A. Osuka, D. Kim, Relationship between two-photon absorption and the  $\pi$ -conjugation pathway in porphyrin arrays through dihedral angle control. *J. Am. Chem. Soc.* **128**(5), 1700–1704 (2006)
85. J.E. Raymond, A. Bhaskar, T. Goodson III, N. Makiuchi, K. Ogawa, Y. Kobuke, Synthesis and two-photon absorption enhancement of porphyrin macrocycles. *J. Am. Chem. Soc.* **130** (51), 17212–17213 (2008)
86. M. Velusamy, J.-Y. Shen, J.T. Lin, Y.-C. Lin, C.-C. Hsieh, C.-H. Lai, C.-W. Lai, M.-L. Ho, Y.-C. Chen, P.-T. Chou, J.-K. Hsia, A new series of quadrupolar type two-photon absorption chromophores bearing 11, 12-dibutoxydibenzo[a, c]-phenazine bridged amines; their applications in two-photon fluorescence imaging and two-photon photodynamic therapy. *Adv. Funct. Mater.* **19**(15), 2388–2397 (2009)
87. C. Wu, C. Szymanski, Z. Cain, J. McNeill, Conjugated polymer dots for multiphoton fluorescence imaging. *J. Am. Chem. Soc.* **129**(43), 12904–12905 (2007)
88. Q. Zheng, G. Xu, P.N. Prasad, Conformationally restricted dipyrromethene boron difluoride (BODIPY) dyes: highly fluorescent, multicolored probes for cellular imaging. *Chem. Eur. J.* **14**, 5812–5819 (2008)
89. S. Zeng, X. Ouyang, H. Zeng, W. Ji, Z. Ge, Synthesis, tunable two and three-photon absorption properties of triazine derivatives by branches. *Dyes Pigm.* **94**(2), 290–295 (2012)
90. T.-C. Lin, Y.-H. Lee, B.-R. Huang, C.-L. Hu, Y.-K. Li, Two-photon absorption and effective optical power-limiting properties of small dendritic chromophores derived from functionalized fluorene/oxadiazole units. *Tetrahedron* **68**(25), 4935–4949 (2012)

91. Y. Jiang, Y. Wang, J. Hua, J. Tang, B. Li, S. Qian, H. Tian, Multibranched triarylamine end-capped triazines with aggregation induced emission and large two-photon absorption cross-sections. *Chem. Commun.* **46**, 4689–4691 (2010)
92. R. Castro-Beltran, G. Ramos-Ortiz, C.K.W. Jim, J.L. Maldonado, M. Häußler, D. Peralta-Dominguez, M.A. Meneses-Nava, O. Barbosa-Garcia, B.Z. Tang, Optical nonlinearities in hyperbranched polyyne studied by two-photon excited fluorescence and third-harmonic generation spectroscopy. *Appl. Phys. B* **97**, 489–496 (2009)
93. Y. Wan, L. Yan, Z. Zhao, X. Ma, Q. Guo, M. Jia, P. Lu, G. Ramos-Ortiz, J.L. Maldonado, M. Rodríguez, A. Xia, Gigantic two-photon absorption cross sections and strong two-photon excited fluorescence in pyrene core dendrimers with fluorene/carbazole as dendrons and acetylene as linkages. *J. Phys. Chem. B* **114**, 11737–11745 (2010)
94. H. Xiao, C. Mei, B. Li, N. Ding, Y. Zhang, T. Wei, Synthesis, solvatochromism and large two-photon absorption cross-sections of water-soluble dipicolinate-based pyridinium salts. *Dyes Pigm.* **99**, 1051–1055 (2013)
95. M. Drobizhev, A. Karotki, A. Rebane, Dendrimer molecules with record large two-photon absorption cross section. *Opt. Lett.* **26**(14), 1081–1083 (2001)
96. N. Rendón, A. Bourdolle, P.L. Baldeck, H. Le, C. Andraud, S. Brasselet, C. Copéret, O. Maury, Bright luminescent silica nanoparticles for two-photon microscopy imaging via controlled formation of 4,4'-diethylaminostyryl-2, 2'-bipyridine Zn(II) surface complexes. *Chem. Mater.* **23**, 3228–3236 (2011)
97. A. Narayanan, O. Varnavski, O. Mongin, J.-P. Majoral, M. Blanchard-Desce, T. Goodson III, Detection of TNT using a sensitive two-photon organic dendrimer for remote sensing. *Nanotechnology* **19**, 115502 (2008). (6 p)
98. H. Wang, T.B. Hufft, D.A. Zweifelt, W. Het, P.S. Lowt, A. Weit, J.-X. Cheng, In vitro and in vivo two-photon luminescence imaging of single gold nanorods. *PNAS* **102**(4), 15752–15756 (2005)
99. D.R. Warren, R. Zipfel, R. Williams, S. Clark, M. Bruchez, F. Wise, W. Webb, Water-soluble quantum dots for multiphoton fluorescence imaging in vivo. *Science* **30**, 1434–1436 (2003)

Contemporary Optoelectronics

Materials, Metamaterials and Device Applications

Shulika, O.; Sukhoivanov, I. (Eds.)

2016, X, 234 p. 121 illus., 66 illus. in color., Hardcover

ISBN: 978-94-017-7314-0